

The present status of the VIRGO Central Interferometer*

F Acernese^{1,2}, P Amico³, N Arnaud^{4,5}, C Arnault^{4,5}, D Babusci⁶,
 G Ballardini⁷, F Barone^{1,8}, M Barsuglia^{4,5}, F Bellachia^{4,5}, J L Beney^{4,5},
 R Bilhaut^{4,5}, M A Bizouard^{4,5}, C Boccara⁹, D Boget¹⁰, F Bondu¹¹,
 C Bourgoin¹², A Bozzi¹², L Bracci^{13,14}, S Braccini⁷, C Bradaschia⁷,
 A Brillat¹¹, V Brisson^{4,5}, D Buskulic¹⁰, J Cachena¹¹, G Calamai^{13,14},
 E Calloni^{1,2}, P Canitrot^{4,5}, B Caron¹⁰, C Casciano⁷, C Cattuto³,
 F Cavalier^{4,5}, S Cavaliere^{1,2}, R Cavaliere⁷, R Cecchi⁷, G Cella⁷,
 R Chiche^{4,5}, F Chollet¹⁰, F Cleva¹¹, T Cokelaer¹¹, S Cortese¹²,
 J P Coulon¹¹, E Cuoco^{13,14}, S Cuzon^{4,5}, V Dattilo⁷, P Y David¹⁰,
 M Davier^{4,5}, M De Rosa^{1,2}, R De Rosa^{1,2}, M Dehamme^{4,5}, L Di Fiore¹,
 A Di Virgilio⁷, P Dominici^{13,14}, D Dufournaud¹⁰, C Eder^{4,5}, A Eleuteri^{1,15},
 D Enard¹², A Errico¹², G Evangelista^{1,2}, L Fabbroni^{13,14}, H Fang⁶,
 I Ferrante⁷, F Fidicaro⁷, R Flaminio¹⁰, J D Fournier¹¹, L Fournier¹⁰,
 S Frasca^{16,17}, F Frasconi⁷, L Gammaitoni³, P Ganau¹⁸, F Garufi¹,
 M Gaspard^{4,5}, G Gennaro⁷, L Giacobone¹⁰, A Giazotto⁷, G Giordano⁶,
 C Girard¹⁰, G Guidi^{13,14}, H Heitmann¹¹, P Hello^{4,5}, R Hermel¹⁰,
 P Heusse^{4,5}, L Holloway⁷, M Iannarelli⁶, J M Innocent¹¹, E Jules^{4,5},
 P La Penna⁷, J C Lacotte¹⁰, B Lagrange¹⁸, M Leliboux⁹, B Lieunard¹⁰,
 O Lodygenski^{4,5}, T Lomtadze⁷, V Lorient⁹, G Losurdo^{13,14}, M Loupias¹¹,
 J M Mackowski¹⁸, E Majorana^{16,17}, C N Man¹¹, B Mansoux^{4,5},
 F Marchesoni³, P Marin^{4,5}, F Marion¹⁰, J C Marrucho^{4,5}, F Martelli^{13,14},
 A Masserot¹⁰, L Massonnet¹⁰, S Mataguez¹², M Mazzoni^{13,14},
 M Mencik^{4,5}, C Michel¹⁸, L Milano^{1,2}, J L Montorio¹⁸, N Morgado¹⁸,
 B Mours¹⁰, P Mugnier¹⁰, L Nicolosi⁷, J Pacheco¹¹, C Palomba^{16,17},
 F Paoletti⁷, A Paoli¹², A Pasqualetti¹², R Passaquieti⁷, D Passuello⁷,
 M Perciballi^{16,17}, L Pinard¹⁸, R Poggiani⁷, P Popolizio¹², T Pradier^{4,5},
 M Punturo³, P Puppo^{16,17}, K Qipiani¹, J Ramonet¹⁰, P Rapagnani^{16,17},
 A Reboux^{4,5}, T Regimbau¹¹, V Reita⁹, A Remillieux¹⁸, F Ricci^{16,17},
 F Richard¹², M Rippepe^{13,14}, P Rivoirard^{4,5}, J P Roger⁹, J P Scheidecker¹¹,
 S Solimeno^{1,2}, R Sottile¹⁰, R Stanga^{13,14}, R Taddei⁷, M Taurigna^{4,5},
 J M Teuler¹², P Tournenc¹¹, H Trinquet¹¹, E Turri⁶, M Varvella¹,
 D Verkindt¹⁰, F Vetrano^{13,14}, O Veziant¹⁰, A Viceré⁷, J Y Vinet¹¹,
 H Vocca³, M Yvert¹⁰ and Z Zhang¹²

¹ Istituto Nazionale di Fisica Nucleare, sez. Napoli, Complesso Universitario di Monte S Angelo, Via Cintia, 80126 Napoli, Italy

² Dipartimento di Scienze Fisiche, University of Napoli, 'Federico II', Complesso Universitario di Monte S Angelo, Via Cintia 80126 Napoli, Italy

³ Istituto Nazionale di Fisica Nucleare, sez. Perugia and University of Perugia, Via A Pascoli 06123 Perugia, Italy

* Presented by L Di Fiore for the VIRGO Collaboration.

- ⁴ Laboratoire de l'Accelérateur Lineaire, Orsay, France
⁵ Université de Paris Sud, BP 34, 91898, France
⁶ INFN Laboratori Nazionali di Frascati, Via E Fermi 40, 00044 Frascati (Roma) Italy
⁷ Istituto Nazionale di Fisica Nucleare, Sez. Pisa, Via Livornese 1291, 56010 S Piero A Grado (Pi), Italy
⁸ Dipartimento di Scienze Farmaceutiche, University of Salerno, Via Ponte Don Melillo, 84084 Fisciano, Salerno, Italy
⁹ ESPCI, 10 Rue Vauquelin, 75005 Paris, France
¹⁰ LAPP, Chemin de Bellevue, BP 110, 74941, Annecy-le Vieux Cedex, France
¹¹ Observatoire de la Cote d'Azur, BP 4229, 06034 Nice Cedex 4, France
¹² EGO, Traversa H di via Macerata, 56021, S Stefano a Macerata (Pi), Italy
¹³ Istituto Nazionale di Fisica Nucleare, Sez. Firenze Largo E Fermi 2, 50125 Firenze, Italy
¹⁴ University of Urbino, Via S Chiara, 27, 61029, Urbino, Italy
¹⁵ Dipartimento di Matematica Applicata ed Informatica, University of Napoli, 'Federico II', Complesso Universitario di Monte S Angelo, Via Cintia, 80126 Napoli, Italy
¹⁶ Istituto Nazionale di Fisica Nucleare, Sez. Roma I, Piazzale Aldo Moro 5, 00185 Roma, Italy
¹⁷ Dipartimento di Fisica, University of Roma 'La Sapienza', Piazzale Aldo Moro 5, 00185 Roma, Italy
¹⁸ IPNL, 43 Boulevard du 14 Novembre 1918, 69622 Villeurbanne Cedex, Lyon, France

E-mail: luciano.difiore@na.infn.it

Received 4 October 2001, in final form 14 November 2001

Published 11 March 2002

Online at stacks.iop.org/CQG/19/1421

Abstract

The VIRGO Central Interferometer (CITF) is a short suspended interferometer operated with the central area elements of the VIRGO detector. The main motivation behind the CITF is to allow the integration and debugging of a large part of the subsystems of VIRGO while the construction of the long arms of the antenna is being completed. This will permit a faster commissioning of the full-size antenna. In fact, almost all the main components of the CITF, with the exception of the large mirrors and a few other details, are the same as those to be used for the full-size detector. In this paper the present status of the VIRGO CITF is reported.

PACS number: 0480N

1. Introduction

VIRGO is a French–Italian collaboration for the construction of a 3 km long interferometric GW detector [1, 2]. The antenna is essentially a Michelson interferometer with Fabry–Perot cavities of finesse $F = 50$ in the arms and power recycling. A monolithic low power Nd:YAG laser and an injection-locked, high power, diode-pumped Nd:YAG laser in a master/slave configuration, actively amplitude and frequency stabilized, delivers a power of 20 W to the interferometer that, with a power recycling factor of 50, yields a stored power of more than 10 kW in the FP cavities. Before lighting the interferometer, the laser beam is filtered by a 144 m long input mode cleaner (IMC), which is a triangular cavity that filters geometrical, frequency and amplitude fluctuations.

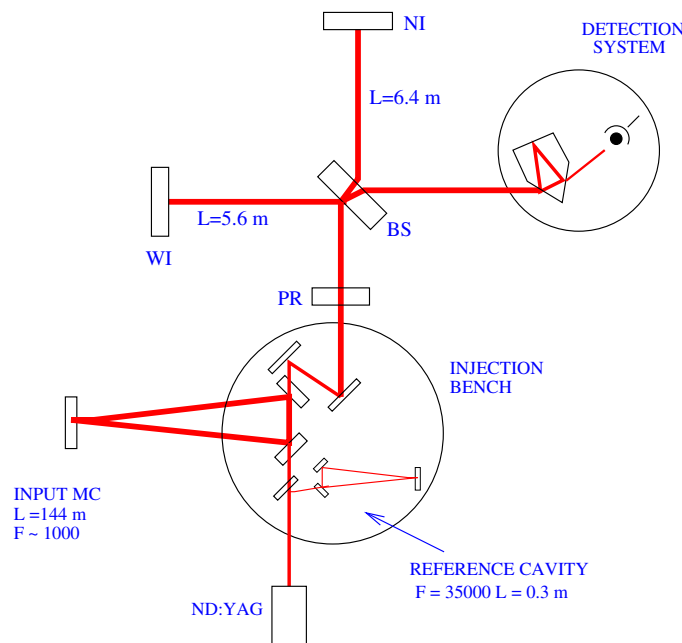


Figure 1. Sketch of the Virgo Central Interferometer.

The construction of VIRGO is under way outside Cascina, a small town close to Pisa. At the moment, some of the infrastructure, as for example the buildings at the ends of the arms that will contain the two end mirrors of the FP cavities, are still to be completed. The completion of assembly and integration is expected for the second half of 2002, whereas the commissioning of the whole interferometer should start at the beginning of 2003. Regarding the vacuum system, the construction of the west arm is completed and the first 300 m tube section has already been tested for leaks and performance after bake-out at 150 °C; the total pressure at 24 °C is about 8×10^{-10} mbar with good residual gas composition. The completion of the north arm is expected by June 2002. The vacuum towers of the central area have also been pumped and tested, with the super-attenuators assembled inside, with satisfactory results. Details on the other sub-systems are given in section 2.

In the central area of VIRGO, there is a device presently in operation called the ‘central interferometer’. It is essentially a short Michelson interferometer with power recycling. All the main components of the device are those of the final VIRGO, with the only exception of the large mirrors and a few minor details. The main motivation behind operating such an interferometer is the possibility of integrating and debugging the various subsystems of VIRGO while the construction of the long arms is being completed. It also allows us to define and test many of the procedures for the control and locking on the interferometer. In the end, the work performed on the CITF will speed up the commissioning of the full-size antenna.

2. The central interferometer

A sketch of the CITF is shown in figure 1. The injection system includes the laser source, and the input mode cleaner (IMC), a long triangular cavity with the far mirrors placed 144 m

apart and the corner placed on an injection bench that also supports the pre-stabilization cavity and the input telescope for matching the beam with the interferometer. Both the IMC and the injection bench are suspended on a shorter version of the super-attenuators described below (three passive filters instead of five).

The main optical elements of the interferometer, the recycling mirrors (RM), the beam splitter (BS) and the mirrors in the north (NI) and west (WI) arms, are suspended on long SA chains. These regular-size suspensions are multi-stage seismic isolators [3], called super-attenuators (SA). Each SA is comprised of a pre-isolation stage, which is essentially an inverted pendulum supporting the top stage of the suspension, a cascade of passive isolation stages and a lower part with an intermediate stage, called a 'marionetta', from which the test mass of the suspension (that is one of the optical elements of the interferometer) and an aluminium mass, called the 'reference mass', are suspended. The SA permits us to push the lower frequency of the VIRGO sensitivity curve down to about 4 Hz. To control the test mass movement, forces can be applied on the SA at various levels [4]. There are three coils attached to the ground acting on the top stage (used for inertial damping and DC control). Four coils (two horizontal and two vertical) are mounted on legs attached to the last passive filter and act on four magnets glued on the arms of the marionetta; this set-up allows us to apply a force on the marionetta centre of mass parallel to the interferometer optical axis and torques around axes orthogonal to the optical axis. Four more (horizontal) coils are attached to the reference mass acting on four magnets directly attached to the back of the test mass. For a detailed description of the status of the suspensions, and their performance as seismic isolators see [3, 5].

As mentioned before, the mirrors are different from the final one; in particular they are smaller in diameter and thickness and have different curvature radii (while all the mirrors of VIRGO are flat with the exception of the end mirrors of the long FP cavities). For this reason, the mirrors are mounted on cylindrical aluminium masses in order to fit with the size and weight of the final (monolithic) mirrors. The last part of the CITF (and of VIRGO) suspended under vacuum, is the detection bench that supports the output mode cleaner (OMC) and several matching optics and photo-detectors, while the main output photo-detector (made up of a set of photo-diodes) is placed on an external bench with other detectors and cameras [6].

The Virgo data acquisition system (DAQ) [9] uses a timing synchronization system based on the GPS signal and collects data under the frame format. The front-end is based on the software running under LynxOS, and on hardware in VME crates. The collection and merging of data are done by a set of software (main frame builders) running on Unix workstations, using a Gigabit Ethernet network with TCP/IP protocol. Data acquisition collects data from three main lines (environment monitoring, detection set-up and suspensions). The resulting frames are currently written on disk and passed to a first prototype of online processing at a rate of 3.5 MB s^{-1} of compressed data. The DAQ system has been installed since the beginning of year 2000 and it is now quite complete and stable.

The assembly and integration of the CITF are already completed and the whole system is under vacuum according to the specifications. The commissioning has been split into two main separate parallel activities, going on simultaneously, involving the injection system and the interferometer.

For the first part, the laser (10 W) has been operative for more than 6000 h performing in agreement with the specifications while the control and locking of the input mode cleaner are being tested. All the details about the present status of the injection system can be found elsewhere [10] in these proceedings.

The second part is the Michelson interferometer itself, with the four test masses attached to the seismic suspensions. At this stage of the commissioning, the interferometer has been

illuminated with an ancillary laser, a commercial monolithic Nd:Yag, because the main laser is still involved in the commissioning of the IMC. Of course this solution allows us to address many issues connected with control and locking, but it is not suitable to evaluate the sensitivity factor as the available power is far too low (~ 160 mW), and the laser itself is too noisy.

One of the most important goals for the CITF is the development and tuning of the servo-system for the control of the position and orientation of test masses and the locking of the interferometer. Due to the extreme complexity of the system and the stringent specifications imposed by the requirement of high sensitivity at frequencies as low as a few hertz, the action of the servo-loops is hierarchically distributed at the different stages of the suspensions (top stage, marionetta and reference mass) with different bandwidths [7, 8], and using error signals provided by both local sensors (position sensors, accelerometers) and interferometer signals.

The first step of the control is the inertial damping (ID). It is three DOF servo systems acting on the top stage of each suspension. The error signal is provided by three accelerometer + three position sensors (for DC control); the goal is to reduce the RMS motion of the top stage and then that of the payload.

The local control system permits control of the position and orientation of the payloads with respect to a local reference frame. The position of the test mass is reconstructed, on six DOF, by analysing the image of a camera looking at the mirror surface. In practice what is recovered is the position of some markers on the test mass surface and of a beam reflected by the mirror itself. The signal is used to damp mirror oscillations and correlate its position to the VIRGO general reference systems; in this way it is possible to realign and superimpose the beams in order to get interference on the output photo-detectors, with a residual angular error of the order of about 10^{-6} rad; that is the starting point for lock acquisition.

Before starting the locking of the CITF, the mechanical transfer function for forces applied with the loop actuators has been measured using a dedicated interferometric device [12–14].

The last step of the control (locking) involves the whole interferometer rather than the single suspensions; the error signals are provided by the global control (GC) system [15] that processes the (DC and demodulated) signals acquired by the output photo detectors and reconstructs the relevant lengths, which are common and differential modes for recycling and Michelson locking, respectively (for the CITF). The role of the global control is to provide the control architecture by switching from lock acquisition mode to normal operation (once the lock is acquired) and to deliver the control signals to the various stages of the different suspensions. Once the interferometer is locked, the angular control servo-loops should be switched from local sensors to global signals to reduce the re-injected noise. The VIRGO GC system is based on two 400 MHz CPUs and provides alignment signals at 500 Hz and locking signals at 10 kHz where the data are received and sent through digital optical links; this system is regularly working for the control of the CITF.

For the tests performed so far, the CITF has been operated as a simple Michelson interferometer by rotating the recycling mirror by an angle large enough so that the cavity is not resonating and the mirror just acts as an attenuator. In this configuration the locking acts on one single DOF (the relative arm lengths) and the correction is applied on either the WI or the NI suspension. For the moment a very simple control scheme has been adopted, where the correction is directly applied on the mirror by acting from the reference mass in the whole band of the servo-loop (DC up to 25 Hz). With this scheme, the interferometer is operated in a stable and robust configuration for runs of more than 20 h. In figure 2, the displacement noise of the CITF is shown. The plot is compared with the estimated contribution of some noise sources. As expected, the detector is limited by seismic noise from DC up to about 1 Hz; the seismic noise used in the plot is computed by taking the seismic noise measured by the accelerometers placed on the top stage of the SA and filtering it with a mathematical

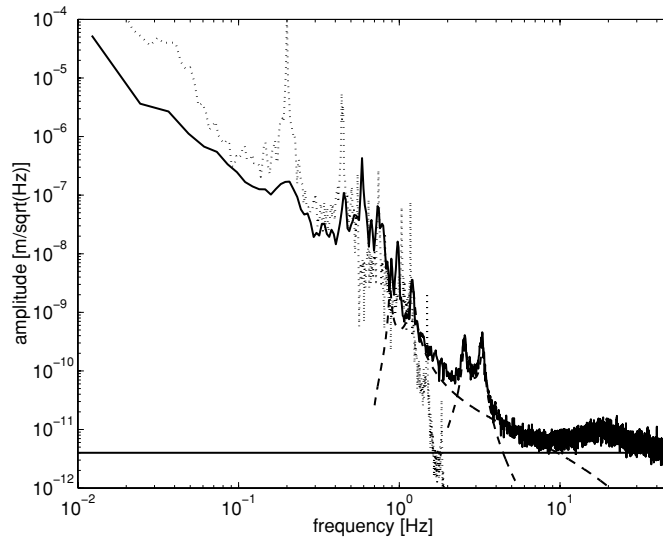


Figure 2. CITF noise spectrum (solid line) compared with the estimated seismic noise (dotted line) and the contribution of angular loops noise (dashed lines); the horizontal line denotes the photo-diode noise level.

model of the pendulum transfer function. The discrepancy at frequency below 500 MHz is due to the usage of a simplified model that does not take into account the zeros of the TF (due to ID) and then gives an over-estimation of the transmitted seismic noise in the ID loop bandwidth. Above 1 Hz, the spectrum is dominated by the noise introduced by angular controls; this is not surprising because the orientation of the mirrors is presently under local control and, at frequencies above the SA normal modes, the error signal is dominated by the position sensor noise (a camera focused at the mirror surface). The situation should be much improved when the 'linear alignment system', which takes the error signals from the much less noisy interferometric signals, is implemented. In the end, above ~ 20 Hz the limit is the photo-diode noise; this depends on the need for a strong amplification of the photo-diode signal for compensating the low laser power and the low transmittance of the recycling mirror out of resonance.

Perhaps the graph shown in figure 3 is more interesting, where for each frequency f , the spectrum integrated from f to high frequency is shown. This allows us to discriminate the contribution of the different peaks to the open-loop RMS mirror relative displacement. We can see that the largest contribution is confined below 100 mHz; the RMS is a few 10^{-8} m between 0.1 and ~ 1 Hz and less than 3×10^{-11} m above 3 Hz. As explained earlier, for each SA, the control loop is distributed at three levels along the suspension chain; this is mainly imposed by the finite dynamics of the coil drivers (~ 140 dB). This limits the maximum force that can be applied directly to the mirror without spoiling the sensitivity of the interferometer at the left corner of the measurement band. For the action on the upper stages (marionetta and top stage) the specification is much relaxed thanks to the mechanical filtering of the coil drivers noise transmitted to the mirror. According to our present design [7], the feedback should be performed acting on the top stage from DC up to a few mHz, from filter 7 up to 4 Hz and from reference mass above. The RMS motion to be corrected by the direct FB on the mirror is less than 3×10^{-11} m, which means that the corresponding coil driver noise limit is 3×10^{-18} m Hz $^{-1/2}$, which is compliant with the low frequency goal sensitivity of VIRGO [16].

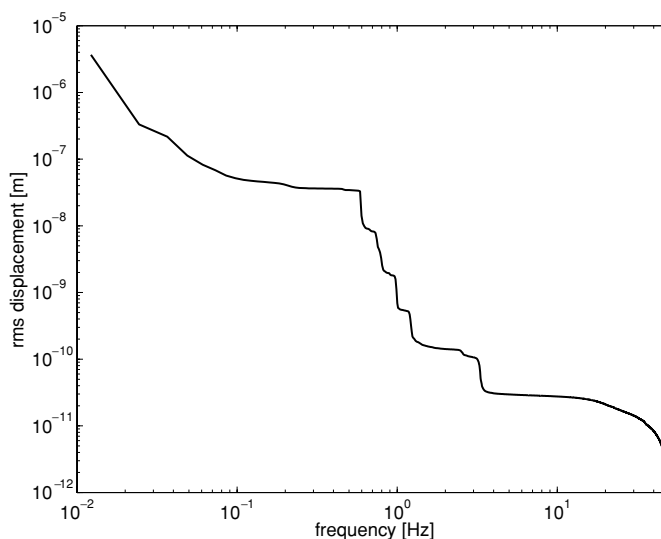


Figure 3. RMS residual motion integrated, for each frequency, from f upward; the large part of the motion is below 100 mHz.

It is worth noting that, above a few Hz, the measured relative motion is presently dominated by sensor noise, and the actual displacement is expected to be smaller by a few orders of magnitude (for further details see [8]).

3. Conclusion

In this paper, a review of the present status of the Virgo CITF is given. The device has been operated as a simple Michelson locked on the dark fringe. The main goals thus achieved are the validation of the suspension performance and the feasibility proof of the control system that acts on the SA with only internal forces. Even more important is the successful integration, from both the hardware and software points of view, of all subsystems involved (data acquisition, global control, local controls, suspension electronics, detection system, etc). Simultaneously, the commissioning of the injection system is quite advanced and tuning of the relative control system is almost completed. The next important topics in the commissioning of the CITF, that are presently under test, are the locking of the recycling cavity, the study and definition of the partition of forces along the SA chains, integration of the linear alignment system and, finally, integration of the interferometer and injection system into a single device. The commissioning of the CITF is expected to be completed during 2002 in order to start the transition to the full-size antenna in 2003.

References

- [1] Virgo Final Design 1997 VIR-TRE-1000-13
- [2] Brillat A for the VIRGO Collaboration 1998 VIRGO - Status Report, November 1997 *2nd E Amaldi Conf. on Gravitational Waves* ed E Coccia, G Veneziano and G Pizzella (Singapore: World Scientific)
- [3] Ballardin G *et al* 2001 *Rev. Sci. Instrum.* **72** 3643
- [4] Passuello D for the VIRGO Collaboration 2001 Controlling the VIRGO mirrors with the superattenuators Talk presented at *4th Edoardo Amaldi Conf. on Gravitational Waves (Perth, Western Australia, 8–13 July 2001)*

-
- [5] Braccini S for the VIRGO Collaboration 2002 The VIRGO suspensions *Proc. of the 4th Edoardo Amaldi Conf. on Gravitational Waves (Perth, Western Australia, 8–13 July 2001)* *Class. Quantum Grav.* **19** 1623
 - [6] Flaminio R for the VIRGO Collaboration 2002 The VIRGO detection system *Proc. of the 4th Edoardo Amaldi Conf. on Gravitational Waves (Perth, Western Australia, 8–13 July 2001)* *Class. Quantum Grav.* **19** 1857
 - [7] Barsuglia M *et al* 2000 Definition of band-width and slope of the servo-loop for SA control VIR-NOT-NAP-1390-143
 - [8] Losurdo G for the VIRGO Collaboration 2002 Active controls of the VIRGO Superattenuator *Proc. of the 4th Edoardo Amaldi Conf. on Gravitational Waves (Perth, Western Australia, 8–13 July 2001)* *Class. Quantum Grav.* **19** 1631
 - [9] Verkindt D *et al* 2000 *9th Marcel Grossmann Meeting (Roma 2–8 July 2000)*
 - [10] Bondu F for the VIRGO Collaboration 2002 The VIRGO injection system: laser, long mode cleaner, alignment and locking sequences *Proc. of the 4th Edoardo Amaldi Conf. on Gravitational Waves (Perth, Western Australia, 8–13 July 2001)* *Class. Quantum Grav.* **19** 1829
 - [11] Losurdo G *et al* 2001 *Rev. Sci. Instrum.* **72** 3653
 - [12] Calloni E *et al* 1998 *Rev. Sci. Instrum.* **69** 1882
 - [13] Calbucci V *et al* 2001 First results on TF measurement and payload control on the BS suspension VIR-NOT-NAP-1390-173
 - [14] Calbucci V *et al* 2000 TF measurement and payload control on the WI suspension VIR-NOT-NAP-1390-174
 - [15] Fabien C 2001 Le contrôle global de VIRGO *Mémoire d'Habilitation à Diriger des Recherches LAL*
 - [16] Punturo M 1999 The VIRGO sensitivity curve VIR-NOT-PER-1390-51